

## Influence of colloid particle profile on sentinel lymph node uptake

Eutimio Gustavo Fernández Núñez<sup>a,\*</sup>, Bluma Linkowski Faintuch<sup>a</sup>, Rodrigo Teodoro<sup>a</sup>,  
Danielle Pereira Wiecek<sup>a</sup>, Jose Roberto Martinelli<sup>b</sup>, Natanael Gomes da Silva<sup>a</sup>,  
Claudia E. Castanheira<sup>a</sup>, Renato Santos de Oliveira Filho<sup>c</sup>, Roberto Pasqualini<sup>d</sup>

<sup>a</sup>Radiopharmacy Center, Institute of Energetic and Nuclear Research, Sao Paulo, SP 05508-000, Brazil

<sup>b</sup>Center of Materials Science and Technology, Institute of Energetic and Nuclear Research, Sao Paulo, SP 05508-000, Brazil

<sup>c</sup>Faculty of Medicine, Federal University of Sao Paulo, SP 04020-041, Brazil

<sup>d</sup>CIS bio international, Research and Development, Gif sur Yvette, 91192, France

Received 28 February 2009; received in revised form 8 April 2009; accepted 27 April 2009

### Abstract

**Introduction:** Particle size of colloids employed for sentinel lymph node (LN) detection is not well studied. This investigation aimed to correlate particle size and distribution of different products with LN uptake.

**Methods:** All agents (colloidal tin, dextran, phytate and colloidal rhenium sulfide) were labeled with <sup>99m</sup>Tc according to manufacturer's instructions. Sizing of particles was carried out on electron micrographs using Image Tool for Windows (Version 2.0). Biodistribution studies in main excretion organs as well as in popliteal LN were performed in male Wistar rats [30 and 90 min post injection (p.i.)]. The injected dose was 0.1 ml (37 MBq) in the footpad of the left posterior limb. Dynamic images (0–15 min p.i.) as well as static ones (30 and 90 min) were acquired in gamma camera.

**Results:** Popliteal LN was clearly reached by all products. Nevertheless, particle size remarkably influenced node uptake. Colloidal rhenium sulfide, with the smallest diameter ( $5.1 \times 10^{-3} \pm 3.9 \times 10^{-3}$  μm), permitted the best result [2.72±0.64 percent injected dose (%ID) at 90 min]. Phytate displayed small particles (<15 μm) with favorable uptake (1.02±0.14%ID). Dextran (21.4±12.8 μm) and colloidal tin (39.0±8.3 μm) were less effective (0.55±0.14 and 0.06±0.03%ID respectively). Particle distribution also tended to influence results. When asymmetric, it was associated with biphasic uptake which increased over time; conversely, symmetric distribution (colloidal tin) was consistent with a constant pattern.

**Conclusion:** The results are suggesting that particle size and symmetry may interfere with LN radiopharmaceutical uptake.

© 2009 Elsevier Inc. All rights reserved.

**Keywords:** Technetium colloids; sentinel lymph node; <sup>99m</sup>Tc-dextran; <sup>99m</sup>Tc-phytate; <sup>99m</sup>Tc-colloidal tin; <sup>99m</sup>Tc-colloidal rhenium sulfide

### 1. Introduction

The lymphatic net has many advantages over blood circulation as a transportation route for tumor cells. Capillaries are much wider and flow speeds markedly lower, thus maintaining optimal cell viability. Lymph is very similar to interstitial fluid and thus promotes cell integrity. In addition, the lymph node (LN) is an ideal incubator of cells with long residence times and areas of stagnant fluid, along with access to other nodes and eventually to the bloodstream [1]. For these reasons, lymphatic mapping and sentinel LN

(SLN) biopsy are extensively used to diagnose and define therapeutic strategy for certain modalities of cancer [2].

The SLN is defined as the first LN to receive drainage from a primary tumor. Detection of metastasis in SLN marks the potential spread of tumor cells to other LN, thus changing surgical approach. In contrast, absence of tumor cells in this first location predicts that the following nodes are probably tumor free as well [3,4]. The contribution of this medical technique may be directly related to survival. Negative biopsy in patients with penile cancer is associated with a 90% survival versus just 20–70 % when the opposite is true [5].

SLN biopsy has evolved into standard practice for surgical management of breast and prostate cancer as well as for melanoma [6–8], with gynecological and gastrointestinal malignancies representing additional candidates [9,10].

\* Corresponding author. Tel.: +55 11 31339557.

E-mail address: [eutimiocu@yahoo.com](mailto:eutimiocu@yahoo.com) (E.G.F. Núñez).

Common lymphatic mapping agents for clinical practice are mostly  $^{99m}\text{Tc}$ -labeled colloids and vital dyes, which provide radioactive signaling, color identification or both via the combined method. When such double technique is employed in tandem, the false-negative rate can be substantially decreased [11].

Success rate of SLN detection depends largely on selection of the radiopharmaceutical. Particle size and surface characteristics could influence rate of colloid drainage from the injection site to dermal lymphatic capillaries as well as of phagocytosis by LN macrophages [12], even though a universal drug based on particle size will probably never be developed, as lymphatic irrigation varies among different organs [13].

There are reasons to suspect that in case of abundant flow larger particles are preferable because smaller ones would be quickly washed away beyond the SLN. Conversely, tiny particles are suitable for regions with scant flow [14].

New radiopharmaceuticals already take into account multiple specificities of the lymphoid tissue [15]. However, prediction of clinical behavior on the basis of physical assessment of the particles and tests in animal models has not been often attempted.

The aim of this article was to evaluate the biological performance of four technetium-99m radiopharmaceuticals (dextran, colloidal tin, Phytate and colloidal rhenium sulfide) in a rat model. The hypothesis was that particle size and distribution could be relevant for functional success of the colloids used in sentinel LN detection.

## 2. Materials and methods

### 2.1. Materials

$^{99}\text{Mo}/^{99m}\text{Tc}$  generators were produced on premises (Institute of Energetic and Nuclear Research, IPEN/CNEN-SP, Brazil). Vital dye for combined technique (patent blue V)

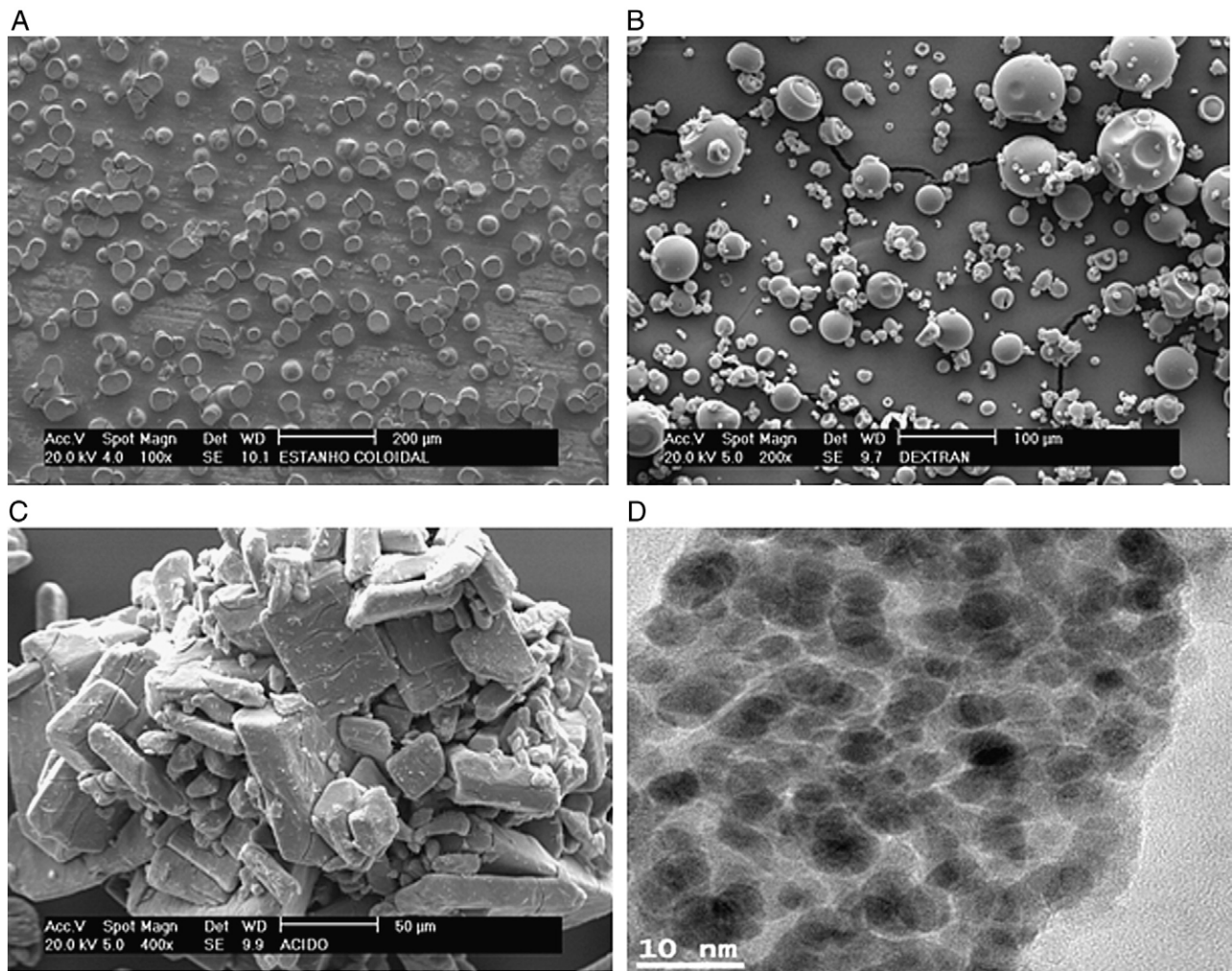


Fig. 1. Electronic microscopy of the four colloids. Colloidal tin (A), dextran 500 (B), phytate (C), colloidal rhenium sulfide (D). Rhenium particles (D) were in the nano range ( $5.1 \pm 3.9 \cdot 10^{-3} \mu\text{m}$ ), whereas dextran and tin were substantially larger. Phytate (C) formed conspicuous agglomerates, albeit particles were quite small ( $<15 \mu\text{m}$ ).

was purchased from Guerbet Prod. Radiológicos, Rio de Janeiro, RJ, Brazil.

Colloidal tin, dextran 500, and phytate kits were produced in house (IPEN/CNEN-São Paulo, Brazil) and colloidal rhenium sulfide kits were a donation from CIS Bio International, France.

Twenty-four young male Wistar EPM-1 rats were provided by the Animal Facility of IPEN-CNEN, weight ranging from 250 to 300 g. They were kept in cages with controlled temperature, humidity and noise, receiving industrialized chow and water ad libitum. All animal studies were performed at the Radiopharmacy Center, IPEN/CNEN, and the protocol was approved by the animal Welfare Ethical Committee.

## 2.2. Analysis of colloidal particles

Size and morphology of the nonradiolabeled particles were examined by transmission (Jeol JEM-2100, Tokyo, Japan) or scanning (Philips XL-30, Eindhoven, The Netherlands) electron microscopy following standard procedures. Sizing of samples was carried out from electron micrographs using the Image Tool for Windows (Version 2.0) software. Dimension was estimated by random Feret diameter.

## 2.3 Preparation of $^{99m}\text{Tc}$ -colloidal tin, $^{99m}\text{Tc}$ -dextran 500 and $^{99m}\text{Tc}$ -Phytate

The three kits were prepared by similar procedures. Briefly, 2 ml of sodium [ $^{99m}\text{Tc}$ ] pertechnetate (740 MBq) were added to the lyophilized product. After 20 min of

incubation at room temperature (23–25°C), the radiopharmaceuticals were ready for use.

## 2.4 Preparation of $^{99m}\text{Tc}$ -colloidal rhenium sulfide

Two milliliters of sterile water for injections were added to the vial B, containing lyophilized stannous salt. Then 0.5 ml of this solution was transferred to vial A, containing rhenium sulfide colloid suspension. Immediately, 1.5 ml of sodium pertechnetate (740 MBq) was added. The reaction was carried out in boiling water bath for 30 min.

## 2.5. Radiochemical control

Radiochemical purity was assessed using paper chromatography. For  $^{99m}\text{Tc}$ -dextran 500 and  $^{99m}\text{Tc}$ -colloidal tin, acetone was chosen for the mobile phase, and Whatman number 3 paper, as stationary phase. For  $^{99m}\text{Tc}$ -Phytate and  $^{99m}\text{Tc}$ -colloidal rhenium sulfide methanol 85%/Whatman 3 and 2-butanone/Whatman 1 systems were respectively utilized.

## 2.6. Popliteal node detection by gamma camera

The animals were anesthetized by means of 25 mg/kg tiletamine hydrochloride associated with 25 mg/kg zolazepam hydrochloride (Zoletil 50, Virbac, São Paulo, Brazil) administered intraperitoneally. Afterwards, 0.1 ml of each radiopharmaceutical was injected in the footpad of the left posterior limb.

Imaging was performed in a Mediso Imaging System, Budapest, Hungary, employing a low-energy, high-resolution

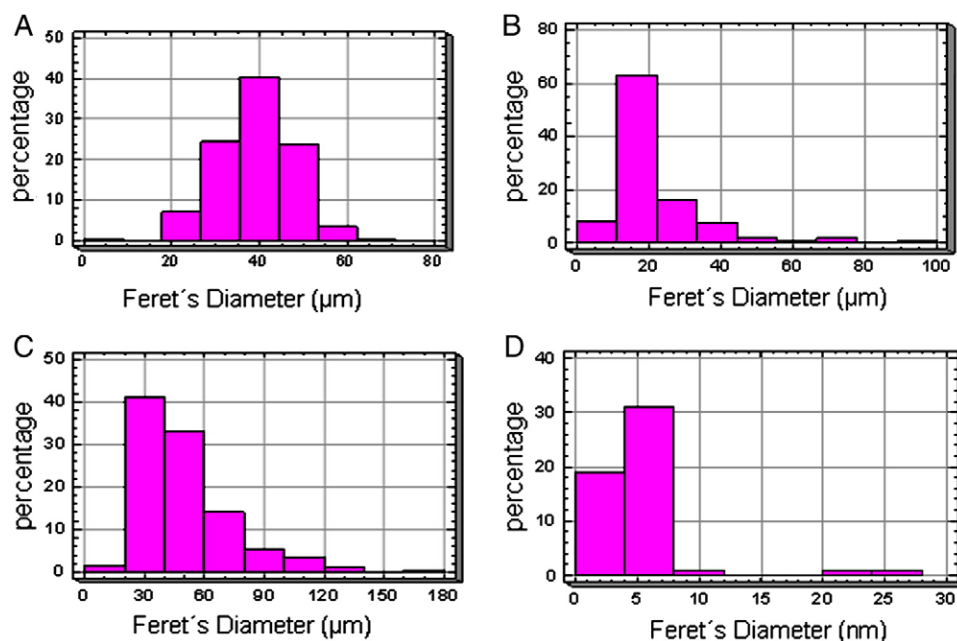


Fig. 2. Frequency histograms for the four colloids. Colloidal tin (A), dextran 500 (B), phytate (C), colloidal rhenium sulfide (D). Only colloidal tin exhibited normal (Gaussian) distribution, all others being asymmetric.

collimator using a  $256 \times 256 \times 16$  matrix size with 20% energy window set at 140 keV. Dynamic studies were conducted for a period of 15 min. Static images were also acquired at 0.5 and 1.5 h post injection (p.i.).

### 2.7. Surgical resection, biodistribution measurements and ex vivo imaging

A second injection in the footpad followed with 0.05 ml vital dye, five minutes before protocol sacrifice time (0.5 and 1.5 h).

The popliteal region was incised permitting access and removal of the popliteal LN. Laparotomy with removal of kidneys and liver was done at the same time. The radioactivity of the specimens was determined by  $\gamma$ -counting using as standard the injected dose of radiotracer. Results

were expressed as percentage of injected dose (%ID) per organ.

Ex vivo imaging analysis of the popliteal LN, kidneys and liver was performed using the syringe with injected dose together allowing the calculation of the region of interest (ROI).

### 2.8. Statistical analysis

Particle size and biological data were analyzed by Statgraphics Plus 5.0 (Statistical Graphics, Fairfax, VA, USA). Standard skewness coefficient was used to measure the symmetry of colloid profiles. One-way analysis of variance (ANOVA) was performed to compare popliteal LN, kidneys and liver uptakes of the products at 0.5 and 1.5 h, followed by post hoc Tukey test. Student's

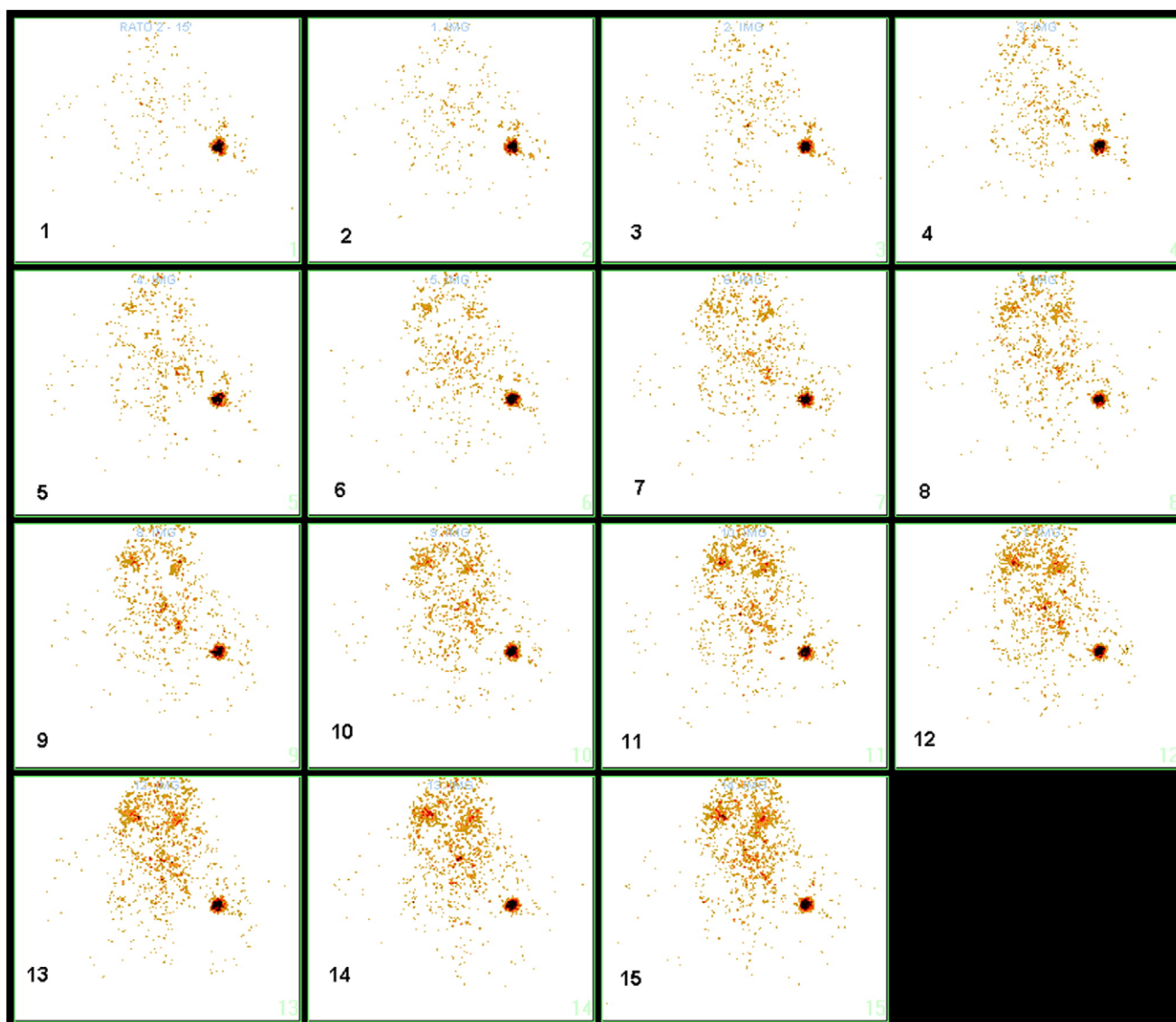


Fig. 3. Dynamic study of  $^{99m}\text{Tc}$ -colloidal tin over the initial 15 min. The dark dot, corresponding to the popliteal LN, can be noticed in all images since the first minute.

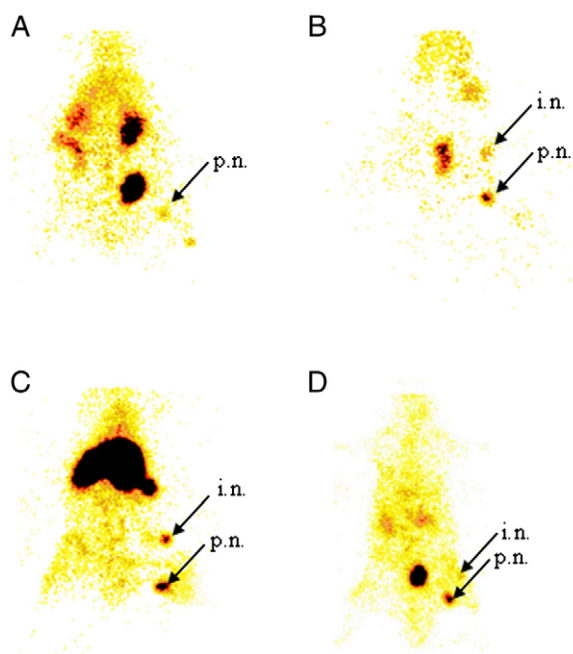


Fig. 4. Static images for all products after 90 min.  $^{99m}\text{Tc}$ -colloidal tin (A),  $^{99m}\text{Tc}$ -dextran 500 (B),  $^{99m}\text{Tc}$ -Phytate (C) and  $^{99m}\text{Tc}$ -colloidal rhenium sulfide (D). p.n., Popliteal node; i.n., inguinal node. Left kidney and bladder (A) or urinary bladder only (B, D) may be identified in the lower part of the animal, not far from the marked LNs. The exception occurred with phytate (C), which elicited strong liver radioactivity, thus confirming hepatic excretion.

*t* test was carried out to identify tissue uptake variability over the time. The adopted significance level ( $\alpha$ ) was  $P < 0.05$ .

### 3. Results

#### 3.1. Colloidal particle morphology

Electron microscopy of nonradiolabeled products showed that phytate particles were small ( $<15 \mu\text{m}$ ), but they formed large agglomerates after solvent evaporation, interfering with size calculation (Fig. 1).

In frequency histograms of particle size (Fig. 2), colloidal tin exhibited symmetric distribution (Standard skewness coefficient =  $-0.178$ ), whereas distribution pattern for other products (dextran, phytate and rhenium sulfide) was asymmetrical — their standard skewness coefficient values

were 15.073, 9.194 and 11.541, respectively. When the values of this statistical parameter are outside the range  $-2$  to  $2$ , the data may depart significantly from a normal distribution (Statgraphics Plus 5.0).

With the exception of rhenium sulfide, with nanometric particles ( $5.1 \pm 3.9 \cdot 10^{-3} \mu\text{m}$ ), dextran displayed the smallest size ( $21.4 \pm 12.8 \mu\text{m}$ ), followed by colloidal tin ( $39.1 \pm 8.32 \mu\text{m}$ ) ( $P = 1.248 \times 10^{-7}$ ). Phytate had large nominal diameter ( $50.0 \pm 23.7 \mu\text{m}$ ), as alluded to, but there was a bias due to agglomerates (Fig. 1).

#### 3.2. Radiochemical controls

High purity levels ( $>95\%$ ) were achieved for all products, thus allowing biological evaluation.

#### 3.3. Gamma camera diagnosis

In dynamic images acquired during the first 15 min, no difference among the markers was documented. Popliteal LN was visualized since the first minute p.i. (Fig. 3). However,  $^{99m}\text{Tc}$ -colloidal tin didn't migrate to the inguinal node, in contrast to all others (Fig. 4).

Static images confirmed renal excretion for  $^{99m}\text{Tc}$ -colloidal tin,  $^{99m}\text{Tc}$ -dextran 500 and  $^{99m}\text{Tc}$ -colloidal rhenium sulfide. Only  $^{99m}\text{Tc}$ -phytate was associated with hepatic metabolism and biliary excretion (Fig. 4).

#### 3.4. Organ biodistribution

Best LN uptake at both times corresponded by far to  $^{99m}\text{Tc}$ -colloidal rhenium sulfide, followed by  $^{99m}\text{Tc}$ -Phytate,  $^{99m}\text{Tc}$ -dextran 500 and  $^{99m}\text{Tc}$ -colloidal tin ( $P = 0.0002$ , ANOVA test for 30 min uptake). Differences between the last two were minor and did not appear on Tukey test at 30 min p.i. (Table 1).

$^{99m}\text{Tc}$ -colloidal rhenium sulfide ( $P = 0.0186$ ),  $^{99m}\text{Tc}$ -phytate ( $P = 0.0017$ ) and  $^{99m}\text{Tc}$ -dextran 500 ( $P = 0.0080$ ) increased LN uptake between 0.5 and 1.5 h, by, respectively, 2.4-, 3.71- and 3.72-fold. No change occurred with  $^{99m}\text{Tc}$ -colloidal tin ( $P = 0.6300$ , nonsignificant) (Table 1).

Higher kidney values were reached by  $^{99m}\text{Tc}$ -colloidal rhenium sulfide and  $^{99m}\text{Tc}$ -colloidal tin, both after 0.5 h ( $P = 0.0116$ ) and 1.5 h ( $P = 0.0001$ ), when compared to the other molecules (Table 1). However, for the same product, no difference was detected in the two time points.

Table 1  
Biodistribution of  $^{99m}\text{Tc}$  radiopharmaceutical in *Wistar* rats

Organ	Lymph node		Kidneys		Liver	
	0.5	1.5	0.5	1.5	0.5	1.5
$^{99m}\text{Tc}$ -colloidal tin	0.04±0.03	0.06±0.03	0.69±0.17	1.02±0.29	0.32±0.10	0.38±0.10
$^{99m}\text{Tc}$ -dextran 500	0.15±0.04	0.55±0.14	0.08±0.06	0.13±0.05	0.04±0.04	0.06±0.05
$^{99m}\text{Tc}$ -phytate	0.27±0.10	1.02±0.14	0.18±0.04	0.16±0.02	13.09±1.94	22.04±1.41
$^{99m}\text{Tc}$ -colloidal rhenium sulfide	1.13±0.32	2.72±0.64	0.94±0.49	0.91±0.05	0.74±0.26	2.36±0.93

Data are expressed as percentage of % injected dose per tissue±standard deviation ( $n=3$ ).

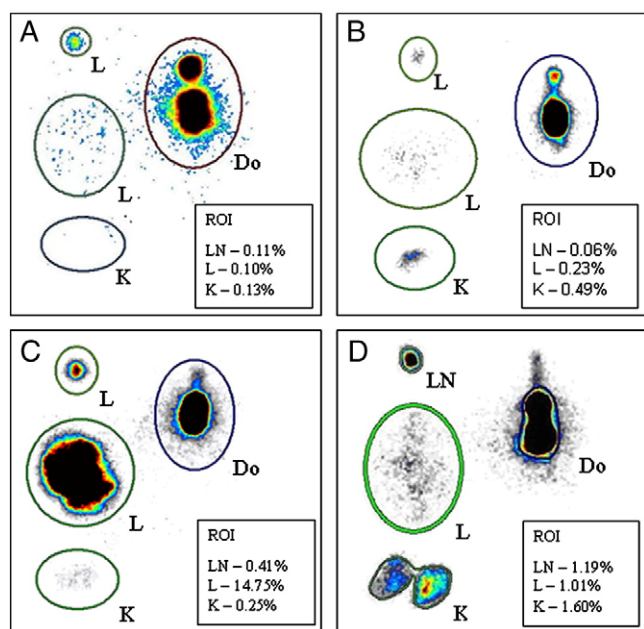


Fig. 5. Ex vivo imaging analysis. ROI uptakes are expressed as a percentage of the injected dose. Dextran 500 (A), colloidal tin (B), phytate (C), colloidal rhenium sulfide (D). L, liver; K, kidneys; Do, dose.

Liver uptake was low for all molecules excluding  $^{99m}\text{Tc}$ -Phytate, which exhibited high percentage in this organ, both at 0.5 and 1.5 h. Liver retention of the  $^{99m}\text{Tc}$ -Phytate increased 1.68-fold ( $P=0.0029$ ) between 0.5 and 1.5 h.

### 3.5. Ex vivo imaging

The ex vivo radioactivity quantification in LN, kidneys and liver by mean of the ROI for all radiocolloids were in accordance with the observed results in biodistribution study at 30 (Fig. 5) and 90 min p.i.

## 4. Discussion

Radiopharmaceuticals for SLN should promptly migrate from the injection site, reach the target and remain there without substantial spill over [16]. Other LNs should remain clean, and contamination of blood vessels should not occur. In synthesis, they should concentrate inside the node, with minimal radioactivity in the other tissues [17].

Biological assessment of popliteal LN by using the combination of radiopharmaceuticals and blue dye in mouse and rat model is well established [12,17,18]. Lymphatic drainage from footpad of mice and rats appear to be exclusively into the popliteal LN, behind the knee. The popliteal LN is relatively large and is easy to find that it is possible to locate and remove [19].

The four products considered in this study are radiocolloids. These radiopharmaceuticals are cleared by lymphatic drainage to SLN, by passive diffusion, with a speed that is inversely proportional to the particle size [20]. Once

inside the LN, they are retained by two main mechanisms, phagocytosis and nonspecific mechanical trapping [21]. Nevertheless, particle size should not be too small or nodal retention of the particle could be compromised [22].

Despite its pharmacologic importance, particle size is overlooked in most protocols. Even products with the same brand and supplier may undergo change of particle size from batch to batch. It is worth mentioning that colloid and radiocolloid dimensions can be controllable by manipulating the conditions under which such colloids form [14].

Success of the SLN technique hinges not only on molecular properties of the radiopharmaceutical but also on surgical skills and injection routine.

With regard to the first variable,  $^{99m}\text{Tc}$  sulfur colloid has been used in the United States, and both  $^{99m}\text{Tc}$  Nan colloid and  $^{99m}\text{Tc}$  rhenium colloid have been used in Europe. In Japan,  $^{99m}\text{Tc}$  tin colloid,  $^{99m}\text{Tc}$  albumin and  $^{99m}\text{Tc}$  phytate are available for sentinel node biopsy [23]. As here indicated, each agent is endowed with specific properties which have to be tailored to different clinical circumstances.

In Japan and several other countries, large-particle tin colloid was popular at first for breast cancer patients, but since nodal uptake was relatively poor because of the large particle size, small-particle tin colloid, phytic acid and rhenium colloid were progressively introduced.

Timing of the injection deserves attention as well. If a large-particle preparation such as tin colloid is preferred, it is administered 3–15 h before surgery because of slow migration [24].

Delay to reach the popliteal LN was not an end point in the present model, because small animals with nearby injection sites are not appropriate for such observation. Nevertheless, speedier access might have played a role in the more remarkable LN uptake of small particles (Table 1 and Fig. 2).

A hitherto unreported finding that will require further studies, was the relationship between symmetry of particle size profile and change in uptake over time. In the case of colloidal tin, constant uptake coincided with symmetric distribution of colloid particle size. The contrary occurred when products displayed asymmetric distribution (dextran 500, Tc-phytate and colloidal rhenium sulfide). Such biphasic uptake pattern can be ascribed to the hypothesis of small particles reaching the LN first, followed by a second wave of larger ones. Additional studies should be performed taking into consideration the radiocolloid particle profile to confirm this result because some radiopharmaceuticals for SLN detection have shown differences in their particle profiles before and after radiolabeling. However, nonradiolabeled and radiolabeled particles profile showed similar behavior respect with symmetry [25].

Excretion mechanism is not a negligible detail, particularly for nodes and tumors located in the immediate neighborhood of excretory routes. Disappointing or misleading imaging results are a distinct possibility, when prostate or endometrial cancers are analyzed by SLN

procedure with the help of agents with renal disposal [26,27].  $^{99m}\text{Tc}$ -phytate, mainly eliminated by hepatic metabolism, could be an option for such malignancies (Fig. 4C).

In synthesis, development of new radioactive agents for SLN should obviously focus biochemical specificities of lymphoid tissue, but without missing physiological repercussions of particle size and distribution.

## 5. Conclusion

The results are suggesting that particle size and profile of the colloids used as radiopharmaceuticals may interfere with sentinel LN uptake. Rat model is sensitive animal model to study these radiotracer properties. Such features should be taken in account when new radiopharmaceuticals, or novel applications for existing drugs, are being examined.

## Acknowledgments

The authors are indebted to the National Commission for Nuclear Energy (CNEN, São Paulo, Brazil) and the International Atomic Energy Agency (IAEA, Vienna, Austria) for scientific grants. The first author gratefully acknowledges Relma Tavares de Oliveira, for the inspiration to write this paper. The team of authors is also grateful to Nildemar A. M. Ferreira for his assistance in electron microscopy analysis.

## References

- [1] Tobler NE, Detmar M. Tumor and lymph node lymphangiogenesis — impact on cancer metastasis. *J Leukoc Biol* 2006;80:691–6.
- [2] Tsopelas C, Bevington E, Kollias J, Shibli S, Farshid G, Coventry B, et al.  $^{99m}\text{Tc}$ –Evans blue dye for mapping contiguous lymph node sequences and discriminating the sentinel lymph node in an ovine model. *Ann Surg Oncol* 2006;13(5):692–700.
- [3] Koyama T, Tsubota A, Nariiai K, Yoshikawa T, Mitsunaga M, Sumi M, et al. Detection of sentinel nodes by a novel red-fluorescent dye, ATX-S10Na (II), in an orthotopic xenograft rat model of human gastric carcinoma. *Lasers Surg Med* 2007;39:76–82.
- [4] Chen SL, Iddings DM, Scheri RP, Bilchik AJ. Lymphatic mapping and sentinel node analysis: current concepts and applications. *CA Cancer J Clin* 2006;56:292–309.
- [5] Luciani A, Itti E, Rahmouni A, Meignan M, Clement O. Lymph node imaging: basic principles. *Eur J Radiol* 2006;58:338–44.
- [6] Aarsvold JN, Alazraki NP. Update on detection of sentinel lymph nodes in patients with breast cancer. *Semin Nucl Med* 2005;35:116–28.
- [7] Dancey AL, Mahonb BS, Rayatt SS. A review of diagnostic imaging in melanoma. *J Plast Reconstr Aesthet Surg* 2008;61(11):1275–83.
- [8] Meinhardt W. Sentinel node evaluation in prostate cancer. *EAU-EBU Update Series* 2007;5(6):223–31.
- [9] Lambaudie E, Collinet P, Narducci F, Sonoda Y, Papageorgiou T, Carpentier P, et al. Laparoscopic identification of sentinel lymph nodes in early stage cervical cancer Prospective study using a combination of patent blue dye injection and technetium radiocolloid injection. *Gynecol Oncol* 2003;89:84–7.
- [10] Yanagita S, Natsugoe S, Uenosono Y, Arigami T, Arima H, Kozono T, et al. Detection of micrometastases in sentinel node navigation surgery for gastric cancer. *Surg Oncol* 2008;17(3):203–10.
- [11] Noguchi M. Sentinel lymph node biopsy and breast cancer. *Br J Surg* 2002;89:21–34.
- [12] Takagi K, Uehara T, Kaneko E, Nakayama M, Koizumi M, Endo K, et al.  $^{99m}\text{Tc}$ -labeled mannosyl-neoglycoalbumin for sentinel lymph node identification. *Nucl Med Biol* 2004;31:893–900.
- [13] Jinno H, Ikeda T, Matsui A, Kitagawa Y, Kitajima M, Fujii H, et al. Sentinel lymph node biopsy in breast cancer using technetium- $^{99m}$  tin colloids of different sizes. *Biomed Pharmacother* 2002;56:213s–6s.
- [14] Higashi H, Natsugoe S, Uenosono Y, Ehi K, Arigami T, Nakabeppu Y, et al. Particle size of tin and phytate colloid in sentinel node identification. *J Surg Res* 2004;121:1–4.
- [15] Wallace AM, Hoh CK, Darrah DD, Schulteis G, Vera DR. Sentinel lymph node mapping of breast cancer via intradermal administration of Lymphoseek. *Nucl Med Biol* 2007;34:849–53.
- [16] Keshggar MRS, Ell PJ. Clinical role of sentinel-lymph-node biopsy in breast cancer. *Lancet Oncol* 2002;3:105–10.
- [17] Paiva GR, Filho RSO, Ferreira LM, Wagner J, Nogueira SA, Novo NF, et al. Phytate technetium- $^{99m}$  versus dextran 500 technetium- $^{99m}$  in the sentinel lymph node biopsy. *Acta Radiol* 2006;47(1):65–70.
- [18] Nathanson SD, Anaya P, Karvelis KC, Eck L, Havstad S. Sentinel lymph node uptake of two different technetium-labeled radiocolloids. *Ann Surg Oncol* 1997;4(2):104–10.
- [19] Løvik M, Alberg T, Nygaard UC, Samuelsen M, Groeng EC, Gaarder PI. Popliteal lymph node (PLN) assay to study adjuvant effects on respiratory allergy. *Methods* 2007;41(1):72–9.
- [20] Linehan DC, Eberlein TJ. Mechanisms of radiocolloid localization in sentinel node biopsy. *Ann Surg Oncol* 2000;7(2):77.
- [21] Schöder H, Glass EC, Pecking AP, Harness JK, Wallace AM, Hirnle P, et al. Molecular targeting of the lymphovascular system for imaging and therapy. *Cancer Metastasis Rev* 2006;25:185–201.
- [22] Fass L. Imaging and cancer: a review. *Mol Oncol* 2008;2:115–52.
- [23] Koizumi M, Nomura E, Yamada Y, Takiguchi T, Makita M, Iwase T, et al. Radioguided sentinel node detection in breast cancer patients: comparison of  $^{99m}\text{Tc}$  phytate and  $^{99m}\text{Tc}$  rhenium colloid efficacy. *Nucl Med Commun* 2004;25(10):1031–7.
- [24] Ikeda T, Jinno H, Fujii H, Kitajima M. Recent development of sentinel lymph node biopsy for breast cancer in Japan. *Asian J Surg* 2004;27(4):275–8.
- [25] Tsopelas C. Particle size analysis of  $^{99m}\text{Tc}$ -labeled and unlabeled antimony trisulfide and rhenium sulfide colloids intended for lymphoscintigraphic application. *J Nucl Med* 2001;42:460–6.
- [26] Takashima H, Egawa M, Imao T, Fukuda M, Yokoyama K, Namiki M. Validity of sentinel lymph node concept for patients with prostate cancer. *J Urol* 2004;171:2268–71.
- [27] Niikura H, Okamura C, Utsunomiya H, Yoshinaga K, Akahira J, Ito K, et al. Sentinel lymph node detection in patients with endometrial cancer. *Gynecol Oncol* 2004;92(2):669–74.